

# REVIEW OF EMITTANCE DIAGNOSTICS FOR SPACE CHARGE DOMINATED BEAMS FOR AWAKE $e^-$ INJECTOR

Oznur Mete Apsimon<sup>\*†</sup>, Guoxing Xia<sup>†</sup>, The University of Manchester, UK  
 Steffen Doebert, CERN, Switzerland  
 Carsten Welsch<sup>†</sup>, The University of Liverpool, UK

## Abstract

For a low energy, high intensity beam, total beam emittance is dominated by defocusing space charge force. This is most commonly observed in photo-injectors. In this low energy regime, emittance measurement techniques such as quadrupole scans fail as they consider the beam size only depends on optical functions. The pepper-pot method is used for 2D emittance measurements in a single shot manner. In order to measure the beam emittance in space charge dominated regime by quadrupole scans, space charge term should be carefully incorporated into the transfer matrices. On the other hand, methods such as divergence interferometry via optical transition radiation (OTRI), phase space tomography using 1D projections of quadrupole scans can be suitably applied for such conditions. In this paper, the design of a versatile pepper-pot system for AWAKE experiment at CERN is presented for a wide range of bunch charges from 0.1 to 1nC where the space charge force increases significantly. In addition, other aforementioned methods and respective algorithms are introduced as alternative methods.

## INTRODUCTION

Envelope equations summarise the focusing and defocusing forces acting on a space charge dominated beam as shown in Eq.1 [1]. In a photoinjector, electrons emitted by the cathode are promptly accelerated in an RF gun. This provides transverse focusing in an amount proportional to the rate of change in the relativistic gamma factor,  $\gamma'$ , as represented by the second term in the equation. Here, prime indicates the derivative with respect to  $z$ . The third term in the equation of motion represents the cylindrical symmetric external focusing fields such as solenoid fields or ponderomotive rf focusing.

$$\sigma'' + \sigma' \frac{\gamma'}{\beta^2 \gamma} + K_r \sigma - \frac{\kappa_s}{\sigma \beta^3 \gamma^3} - \frac{\epsilon_n^2}{\sigma^3 \beta^2 \gamma^2} = 0 \quad (1)$$

A defocusing space charge force is introduced in the fourth term using the beam perveance,  $\kappa_s = I/2I_0$  where  $I$  is the peak beam current and  $I_0$  is the constant Alfvén current (17 kA). The last term represents the defocusing of normalised rms emittance,  $\epsilon_n$ .

## A VERSATILE PEPPER-POT SYSTEM FOR AWAKE $e^-$ INJECTOR

Emittance will be measured before the injector booster of the AWAKE experiment at CERN [2, 3] in order to set up the beam for routine operation. The beam specifications in Table 1 are considered for the design. The basic design

Table 1: AWAKE Beam Parameters Before the Booster

Parameter	Value
Charge (nC)	0.1-1
Energy (MeV)	5-6
Rep. Rate	10 Hz max, single bunch
Bunch length ( $1\sigma$ , ps)	0.3-4
$\epsilon_n$ ( $1\sigma$ , mm mrad)	1-6

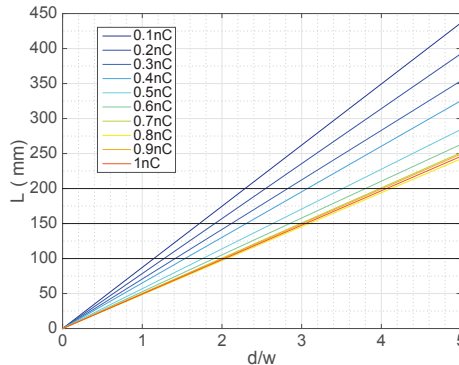


Figure 1: Guidelines for the optimisation of the pepper-pot mask geometry.

criteria for a pepper-pot system are [4–6]: a) Confirmation that the beam-lets are emittance dominated after the mask by using the ratio between space charge and emittance terms of the envelope equation at the location of the screen as in Eq.2, where  $\omega$  is the hole diameter,  $d$  is the centre-to-centre distance between holes and  $L$  is the mask-screen distance. b) Determination of a mask thickness,  $L_s$ , sufficient to stop incoming electrons. c) Preventing beam-lets from overlapping on the screen, where  $\sigma'$  is the rms beam divergence,  $4\sigma'L < d$ , and d) ensuring that position and angle resolutions are comparable,  $\sigma/d = L\sigma'/r_d$ , where  $\sigma$  is the rms beam size and  $r_d$  is the resolution of the detector (CCD camera).

$$R' = \frac{2I}{\gamma^2 I_0} \frac{\omega L}{d \epsilon_n} \quad (2)$$

( $L$ ,  $d/\omega$ ) pairs were determined satisfying the equation assuming  $R' = 0.6$  as shown in Figure 1. Determination of  $d$  and  $\omega$  values relied on the fact that  $\omega$  should be no less than  $100 \mu\text{m}$  to ease the machining process and to provide

<sup>\*</sup> o.mete@lancaster.ac.uk, now affiliated with Lancaster University  
<sup>†</sup> and The Cockcroft Institute, Sci-Tech Daresbury, Warrington, UK

enough transmission for adequate statistics for the data analysis. On the other hand,  $\omega$  should be smaller than  $d$  to resolve the beam and small enough to eliminate the space charge force for each beamlet. Distance between holes,  $d$ , should be smaller than the beam size so that at least five beam-lets can be observed on the screen to ensure the statistical significance of the emittance calculation. Particle distributions at

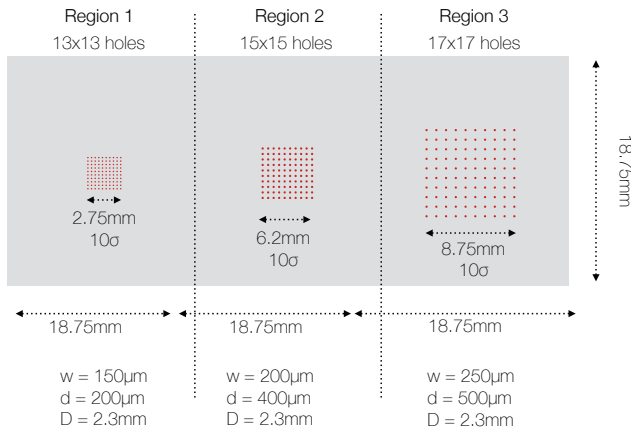


Figure 2: Three geometries on a single Tungsten slab that allows emittance measurement within a range from 0.1 nC to 1 nC.

the mask entrance were obtained from PARMELA [7] simulations. Further tracking through the mask was performed by using a custom tracking script in MATLAB [8] (Figure 3). Particle loss through the thickness of the mask due to particles divergences was taken into account. A 1-2% loss in transmission through the mask was calculated for different beams with 0.1 to 1 nC bunch charge. Design of the mask tested, numerically, using sample beams in steps of 0.1 nC in the given range. Consequently, the values corresponding to three mask designs are summarised in Table 2 relying on the criteria given in Table 3. In Table 2, the simulated emittance measurement results were presented for three mask-screen distances (100, 150 and 200 mm). Figure 4, summarises the calculated emittances for these three  $L$  values; a linear fit used to interpolate the points between the data to find out  $L$  values resulting into the expected emittance values for each case (at different charge values). Optimum ( $\epsilon, L$ ) pairs are marked with bold black dots. According to this, the average optimum distance between the mask and the screen,  $\langle L \rangle$ , is 163 mm. Nevertheless the values calculated for  $L = 150$  mm were marginally better than those for  $\langle L \rangle$ , therefore it is chosen as the baseline for the design.

Tungsten was chosen as the mask material against titanium and graphite; because it has the shortest stopping distance producing about the same level of radiation doses during the electron bombardment as a result of GEANT4 simulations. A geometry as given in Figure 2. Machining of such a mask can be done by pneumatic drilling, laser drilling or electrical discharge machining depending on the accuracy required in terms of draft angle and circularity of the holes and achievable hole aperture to mask thickness ratios.

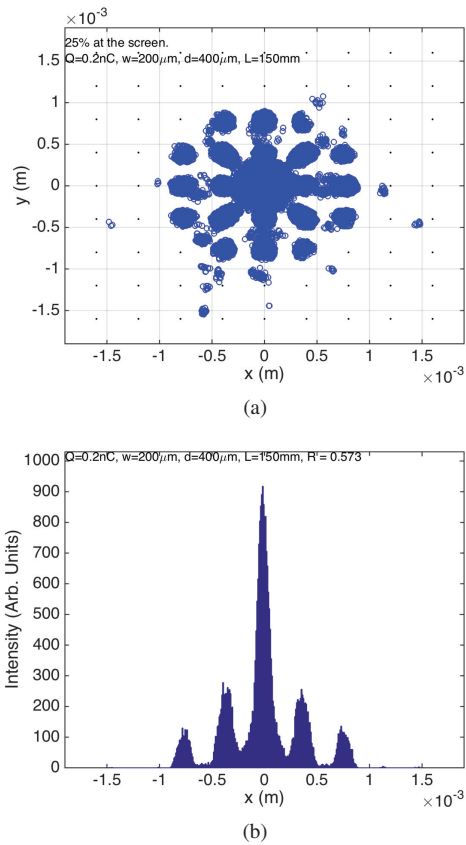


Figure 3: Observables for the baseline charge value of 0.2 nC. a) Beamlets on the screen. b) Projection of the observed image on the x axis.

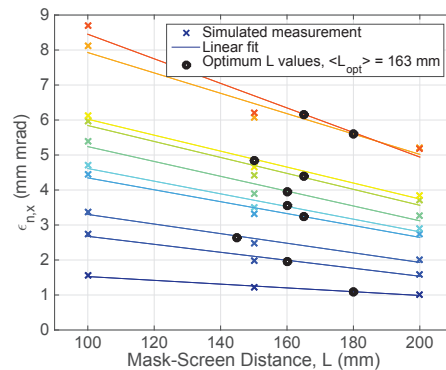


Figure 4: Simulated emittance measurements for three arbitrary  $L$  values and the optimum  $L$  values for each case yielding the expected emittance values.

According to criterion "c)", a certain overlap between the beam-lets are expected in Region 1 where the charge is low and beam size is the smallest in the range of interest. Nevertheless, tracking results were confirmed that the beam-lets can be resolved. Region 2 and 3 are fulfilling the requirement to prevent the beam-lets from overlapping. Table 3 presents a comparison between position and angle resolution (criterion "d)"). Over all the regions considered the position and angle resolution are of the same order of magnitude. Also, it was found in the tracking simulations that mask geometries providing a beam transmission larger than 20% yield

Table 2: Summary of Design for Three Different Regions on the Mask and Values Corresponding to Simulated Measurements

	Charge (nC)	$\sigma_x$ ( $\mu\text{m}$ )	$\omega$ ( $\mu\text{m}$ )	$d$ ( $\mu\text{m}$ )	$\epsilon_{n,sim}$ (mm mrad)	$\epsilon_{n,L=100}$ (mm mrad)	$\epsilon_{n,L=150}$ (mm mrad)	$\epsilon_{n,L=163}$ (mm mrad)	$\epsilon_{n,L=200}$ (mm mrad)
Region 1	0.1	300	150	200	1.09	1.55	1.21	1.15	1.01
Region 2	0.2	400	200	400	1.96	2.74	1.98	1.85	1.60
	0.3	500			2.65	3.37	2.48	2.34	2.00
	0.4	500			3.25	4.44	3.31	3.13	2.74
	0.5	600			3.55	4.72	3.50	3.31	2.91
Region 3	0.6	600	250	500	3.94	5.38	3.90	3.70	3.26
	0.7	600			4.39	5.98	4.43	4.21	3.70
	0.8	600			4.84	6.13	4.67	4.49	3.85
	0.9	800			5.60	8.13	6.07	5.75	5.22
	1.0	800			6.14	8.70	6.20	6.06	5.19

Table 3: Summary of the Assessment Criteria on the Pepper Pot System Design

	Charge (nC)	$R'$	$d$ ( $\mu\text{m}$ )	$4\sigma'L$ ( $\mu\text{m}$ )	$\sigma/d$	$L\sigma'/r_d$	$\epsilon_n/\gamma\sigma$ (mrad)	$\omega/4L_s$ (mrad)	Transmission (%)
Region 1	0.1	0.77	200	243	1.3	3.6	0.3	16	47
Region 2	0.2	0.57	400	246	0.9	3.8	0.4	22	25
	0.3	0.63		264	1.1	4.1	0.4	22	23
	0.4	0.69		270	1.4	4.2	0.5	22	22
	0.5	0.79		288	1.4	4.5	0.5	22	22
Region 3	0.6	0.85	500	312	1.2	5.9	0.5	27	22
	0.7	0.89		336	1.3	5.2	0.5	27	21
	0.8	0.93		366	1.3	5.7	0.6	27	21
	0.9	0.90		336	1.6	5.2	0.5	27	21
	1.0	0.91		360	1.6	5.6	0.6	27	20

expected emittance values when the emittance calculation algorithm is applied to the beamlets produced. The mask thickness (2.3 mm for 6.6 MeV) and hole diameter should be so that the angular aperture  $\omega/L_s$  is at least 4 times larger than the rms beam angle associated with the finite beam emittance  $\epsilon/\gamma\sigma$ .

### ALTERNATIVES: OTRI, TOMOGRAPHY AND MODIFIED QUAD SCAN

Optical transition radiation (OTR) is widely used for beam profile measurement. Analysis of the far field distribution of interfering OTR from two parallel radiating screens (foils) provides information on beam divergence. Beam size can be measured simultaneously from the near field pattern using a beam splitter to obtain  $(x, x')$  and  $(y, y')$  pairs. Empirically the lower limit of divergence measurement is given as  $0.01/\gamma$  [9] where  $\gamma$  is the relativistic Lorentz factor; upper measurement limit depends on the experimental setup. The resolution for the beam size depends on the resolution of the camera and the magnification. Once at least two such pairs are obtained, the algorithm in [10] can be used to calculate the emittance.

One can benchmark the OTRI results against phase space tomography. Tomography in transverse phase space can be performed using the 1D beam projections acquired from a sufficient number of beam profiles, to scan from 0 to  $180^\circ$ , given for different quadrupole settings. A 2D map can be reconstructed by using these 1D projections using the filtered-backprojection algorithm that takes into account the space charge [11].

A study to modify the transverse matrix to include a space charge term and hence correct the quad scan method for high intensity, low energy applications is being carried out.

### CONCLUSIONS AND OUTLOOK

A pepper pot monitor for emittance measurement of beams with significant space charge was designed for the AWAKE experiment to provide single shot measurements. Alternative methods were introduced. OTRI is a novel method which relies on carefully structured algorithms. Tomography reveals more information about the phase space tails. Quadrupole scans can be modified in a way that correctly includes the space charge defocusing.

### ACKNOWLEDGEMENTS

This work was supported by the Cockcroft Institute Core Grant and STFC. Authors also thank to Dr Graeme Burt for his support enabling the continuation of this effort.

### REFERENCES

- [1] L. Serafini Phys. Rev. E 55, 6, p7565, (1997).
- [2] A. Caldwell et al., CERN-SPSC-2013-013 (2013).
- [3] C. Bracco et al., WEPMY019, these proceedings.
- [4] M. Zhang Fermilab-TM-1988 (1996).
- [5] P. Piot et al., PAC97 Proceedings, p2204, (1997).
- [6] S. G. Anderson, PRSTAB 5, 014201 (2002).
- [7] L. M. Young, LA-UR-96-1835 (2005).
- [8] <http://uk.mathworks.com/>
- [9] Private communication with Dr R. Fiorito.
- [10] K. Poorrezai et al., PRSTAB 16, 082801 (2013).
- [11] D. Stratakis et al., PRSTAB 9, 112801 (2006)